

Bilateral Deep Reinforcement Learning Approach for Better-than-human Car Following Model

Tianyu Shi^{1*}, Yifei Ai^{2*}, Omar ElSamadisy¹, Baher Abdulhai¹

Abstract—In the coming years and decades, autonomous vehicles (AVs) will become increasingly prevalent, offering new opportunities for safer and more convenient travel and potentially smarter traffic control methods exploiting automation and connectivity. Car following is a prime function in autonomous driving. Car following based on reinforcement learning has received attention in recent years with the goal of learning and achieving performance levels comparable to humans. However, most existing RL methods model car following as a unilateral problem, sensing only the vehicle ahead. Recent literature, however, Wang and Horn [16] has shown that bilateral car following that considers the vehicle ahead and the vehicle behind exhibits better system stability. In this paper we hypothesize that this bilateral car following can be learned using RL, while learning other goals such as efficiency maximisation, jerk minimization, and safety rewards leading to a learned model that outperforms human driving.

We propose and introduce a Deep Reinforcement Learning (DRL) framework for car following control by integrating bilateral information into both state and reward function based on the bilateral control model (BCM) for car following control. Furthermore, we use a decentralized multi-agent reinforcement learning framework to generate the corresponding control action for each agent. Our simulation results demonstrate that our learned policy is better than the human driving policy in terms of (a) inter-vehicle headways, (b) average speed, (c) jerk, (d) Time to Collision (TTC) and (e) string stability.

I. INTRODUCTION

Inherent system randomness in human-driving behavior [1] creates instability in the traffic system. Shockwaves and stop-and-go have become a primary safety concern and the main cause of traffic jams [2]. Meanwhile, drivers also want to maximize travel efficiency, such as improving average speed and minimizing headway [3]. As a result, a critical question for building an intelligent transportation system (ITS) is how to encourage the vehicle to travel as fast as possible while maintaining safe headway to the leading vehicle and reducing shockwaves.

Autonomous driving technology has been studied for years and started to come to reality with the development of sensors and artificial intelligence (AI). The autonomous driving vehicle could potentially learn to outperform human driving in safety and comfort [3] [4][5]. One major benefit of connected and autonomous vehicle (CAV) is that the randomness in driving behavior can be significantly reduced; thus, the whole

system can be better managed by control algorithms with minimum reaction time.

Car following is a typical driving task. Many models have been developed to mimic human driving behavior [6][7][8]. In traffic flow theory, classic car following models are based on physical knowledge and human behaviors, etc.

For example, the Gipps model considers the driver would estimate the speed based on the vehicle ahead to determine the acceleration or deceleration. The following vehicle's speed is also limited by safety constraints [7]. Another well-known model is the Intelligent driver model (IDM), which models the output acceleration based on the desired velocity, headway, relative speed, and distance to the leading vehicle and by desired velocity in free flow traffic and minimum spacing [8].

In recent years, some studies proposed data driven method to train car following models. He et al. [9] uses K-nearest neighbors (KNN) to find the most likely behavior of vehicles in the car following mode. Some studies also apply supervised learning. Chong et al.[10] uses neural networks to model driver behavior regarding to longitudinal and lateral actions. Zhou et al. [11] focus on capturing and predicting traffic oscillation using recurrent neural networks (RNN) [12].

Although supervised learning methods have shown very good results, it requires hand-collected microscopic car following data which are rare and expensive to collect. Usually, collected data is from human drivers. Some learning methodologies such as Imitation Learning might also lead the trained models to learn some irrational behavior, such as very aggressive or very conservative behaviors from humans. Applications of Reinforcement learning (RL) have rapidly matured in recent research [4][21]. RL has successfully addressed problems such as Go [13] and Atari games [14]. In such framework, RL agents interact with the environment and observe the state and the corresponding reward. They are expected to find the optimal policies that maximize accumulated reward after training. A well-defined reward function usually makes agent's policy converge to the objective we want to achieve. Zhu et al. [15] defines car following models to keep safe distance to the front vehicle and maintain desired speed. Their proposed model can achieve good generalization ability compared to data-driven car following model. However, how to develop better than human driven car following model [8] is still needed for further investigation.

A key question is how will autonomous vehicle affect today's traffic flow? Given the current development of autonomous driving technology, in the traffic flow which involves both human driving and autonomous vehicle (i.e., a mixed autonomy system), there are at least three fundamental challenges:

¹ Tianyu Shi , Omar ElSamadisy, Baher Abdulhai are with the Department of Civil & Mineral Engineering, University of Toronto, 35 St. George Street, Toronto, Ontario, M5S 1A4, Canada. ty.shi@mail.utoronto.ca

² Yifei Ai is with the Department of Mechanical & Industrial Engineering, University of Toronto, 35 St. George Street, Toronto

* Indicates equal contribution

1. How to make AVs perform at least as good as humans, a target below which AVs would be undesirable from a traffic system perspective, and
2. How to make AVs outperform human driving,
3. How to potentially use AVs to influence non-AVs and improve overall traffic system performance.

In this paper we focus on 1 and 2. We address car following to meets efficiency, safety, comfort and traffic stability performance goals.

The previous car following models (CFM) only considers the information from the leading vehicle [5][7][8][15]. Wang and Horn [16] first proposed the bilateral control idea into traffic flow control by adding information about the following vehicle. In their results, they demonstrate better string stability under the bilateral control model (BCM) compared to pure CFM traffic. In terms of chain stability, BCM demonstrates better performance than CFM. However, it's still unknown whether the BCM model will demonstrate better travel efficiency, comfort and safety than CFM. More specifically, BCM model can't learn how to balance and optimize efficiency, safety, comfort and platoon stability together.

In this work, we extend the bilateral control concept into a deep reinforcement learning framework to solve the multi-objective problem. Our experimental results demonstrate that our proposed bidirectional deep reinforcement learning car following model can surpass previous human driving models in terms of (1) inter-vehicle headways, (2) average speed, (3) jerk, (4) safety and (5) string stability.

II. BACKGROUND

A. Markov Decision Process

The learning of optimal policy under a car following task can be formulated as Markov Decision Processes (MDP), which consists of state S , action A , transition function $p(s_{t+1}|s_t, a_t)$ s.t $p(s'|s, a) = \Pr\{s_{t+1} = s'|s_t = s, a_t = a\}$, reward function $r(s, a) = E[r|s_t = s, a_t = a]$. In MDP, a policy function π is a probabilistic mapping from states to the probability of selecting action. The action-value function, (i.e., $\pi(a|s) = \Pr(A_t = a|S_t = s)$) the bellman function [17], can be defined as:

$$Q^\pi(s_t, a_t) = E_{r_t, s_{t+1} \sim E} [r(s_t, a_t) + \gamma E_{a_{t+1} \sim \pi} [Q^\pi(s_{t+1}, a_{t+1})]] \quad (1)$$

B. Q-Learning

Q-learning is one of the most common tabular methods in RL. The state-action value function is estimated by using $Q^\pi(s, a) = E_\pi[r + \gamma Q^\pi(s_1, a_1)|s_0 = s, a_0 = a]$. It uses the following update rule:

$$Q^\pi(s, a) \leftarrow Q^\pi(s, a) + \alpha(r + \gamma \max_{a'} Q(s', a') - Q(s, a)) \quad (2)$$

where α is the learning rate, and γ is the discount factor.

However, this suffers from the curse of dimensionality challenge in systems with large state-action spaces. Thus, other

methods with function approximation are studied by the RL community.

C. Deep Deterministic Policy Gradient

Actor-critic methods are temporal difference (TD) methods that have a separate policy structure independent of the value function [17]. We call the policy function as an actor to select actions. The function that estimates the value function is called a critic. It criticizes the actions selected by the actor.

In this research, we select Deep Deterministic Policy Gradient (DDPG) method [18] to extend for continuous action space. It is an off-policy algorithm whose actor outputs a deterministic action in a continuous space (instead of outputting a probability distribution compared with the vanilla policy gradient).

Similar to other actor-critic methods, it has a policy network μ_θ that outputs a deterministic action. (i.e., $\mu_\theta(s) \in A$ where $s \in S$). And it has a critic estimates the function $Q^*(s, a)$.

Suppose the neural network $Q_\phi(s, a)$ is the approximator of $Q^*(s, a)$ with parameter ϕ , and there is a set of transitions (s, a, r, s', d) . One can optimize the approximator with the following mean-squared Bellman error (MSBE) as the loss function:

$$L(\phi, D) = E[(Q_\phi(s, a) - (r + \gamma(1 - d) \max_{a'} Q_\phi(s', a')))^2] \quad (3)$$

Since finding the maximum is very challenging in the continuous action space, they use $Q_\phi(s', \mu_\theta(s'))$ to approximate $\max_{a'} Q_\phi(s', a')$.

For our policy network, we optimize the approximator by solving:

$$\max_\theta E[Q_\theta(s, \mu_\theta(s))] \quad (3)$$

III. PROBLEM FORMULATION

A. Preliminary

To evaluate the performance of our car-following model, we illustrate the following metrics.

1) Time to collision (TTC): Safety is one of the most important features in driving systems. We use Time to Collision (TTC) to represent safety. TTC represents the time left before two vehicles collide. It is computed as [5] :

$$TTC(t) = \frac{S_{n-1,n}(t)}{\Delta V_{n-1,n}(t)} \quad (4)$$

Here t stands for time; $n - 1$ is the index of the leading vehicle, n is the index of the following vehicle; $S_{n-1,n}(t)$ denotes the clearance distance between the leading and the following vehicles; $\Delta V_{n-1,n}(t)$ represents the relative speed at time t : $V_{n-1}(t) - V_n(t)$.

2) Headway: For our car-following model, we would like the following vehicle to keep a safe and relatively short time headway to the leading vehicle. Time headway is defined as the time it takes for the following vehicle to reach the current location of the leading vehicle. Let $H(t)$ denote the headway at time t , then:

$$H(t) = \frac{S_{n-1,n(t)} + l_{n-1}}{v_n(t)} \quad (5)$$

where l_{n-1} is the length of the leading vehicle, $S_{n-1,n(t)}$ is the clearance distance, $v_n(t)$ is the velocity of the following vehicle.

Additionally, if we look at equation 5 and equation 6, we can find the relationship between TTC and $H(t)$ as following [19]:

$$TTC(t) = -\frac{H(t)v_n(t) - l_{n-1}}{\Delta V_{n-1,n}(t)} \quad (6)$$

In the experiment, we will use average headway over one episode as the metric. We define average headway as follows:

$$\frac{\sum_{t=1}^T H_{n,t}}{T} \quad (7)$$

where $H_{n,t}$ is the headway of vehicle n at time t , T is the total time steps over one episode.

3) Jerk: Comfort is another important element in autonomous driving. We use the jerk to measure comfort. Jerk is defined as:

$$Jerk(t) = \frac{a_n(t) - a_n(t-1)}{\Delta t} \quad (8)$$

where Δt is the time interval between time steps t and $t-1$, $a_n(t)$ is the acceleration of vehicle n at time t .

In the experiment, we use average absolute jerk over one episode as the metric. Since jerk has a positive and negative values, we use the absolute value of jerk:

$$\frac{\sum_{t=1}^T |jerk_{n,t}|}{T} \quad (9)$$

where $jerk_{n,t}$ is the jerk of vehicle n at time t , T is the total timesteps over one episode.

B. Car following models

We will first illustrate some classical car-following models, including both unilateral and bilateral car following models to compare with our bilateral reinforcement learning car-following model.

Given the leading vehicle (L), the current vehicle (C) and follower vehicle (F), A car-following model controls the longitudinal movements for the following vehicle with respect to the leading vehicle's motions.

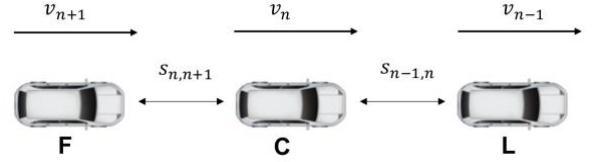


Figure 1. A car following scenario. Illustration of the difference between the previous car-following model and the bilateral control model. 'L' represents the leading vehicle, 'C' represents the current vehicle, 'F' represents the following vehicle.

Several car-following models have been proposed to model the microscopic traffic behavior.

1) *Gipps [1] (unilateral model)*: Gipps is a classical model for modeling driving behavior.

Gipps considers both free-flow mode (without leading vehicle) and car following mode (with the leading vehicle) and takes the minimum velocity of them.

$$v(t + \Delta t) = \min [v + a\Delta t, v_0, v_{safe}(s, v_l)] \quad (10)$$

where v_0 is the desired speed, Δt is the reaction time, and v_{safe} is the safe speed, for which if the leading vehicle suddenly reach to a complete stop, the distance to the leading vehicle needs to guarantee bigger than a minimum gap.

2) *Intelligent driver model (IDM) [8] (unilateral model)*: IDM is a model that models realistic acceleration profiles in the single-lane traffic situations. The following acceleration equation is given below:

$$\dot{v}_c = a \left[1 - \left(\frac{v_c}{v_0} \right)^\delta - \left(\frac{s^*(v_c, \Delta v_c)}{s} \right)^2 \right] \quad (11)$$

where v_0 is the desired velocity for the current vehicle, v_c is the current velocity for the current vehicle, s is the current distance to the leading vehicle, a is the maximum vehicle acceleration.

where $-a \left(\frac{s^*(v_c, \Delta v_c)}{s} \right)^2$ is a breaking term, in which the desired distance s^* is defined as,

$$s^*(v_c, \Delta v_c) = s_0 + \max \left(v_c T + \frac{v_c \Delta v_c}{2\sqrt{ab}}, 0 \right) \quad (12)$$

where s_0 is minimum jam distance, T is the desired time headway, and a is the maximum vehicle's acceleration, b is comfortable deceleration.

3) *Bilateral control model (BCM, bilateral model)* [16]: BCM assumes the vehicle has an additional back sensor. Its control is based on the state of both the leading vehicle and the following vehicle as shown in Figure 1. the controller's equation is given below:

$$a_n = k_d(s_{n-1} - s_n) + k_v(r_{n-1} - r_n) \quad (13)$$

where the s_{n-1} denotes the space between the current vehicle and its leading vehicle; s_n denotes the space between the current vehicle and its follower vehicle. r_{n-1} and r_n denotes the relative speed between the current vehicle to its leading vehicle and its follower vehicle respectively. The k_d and k_v are proportional and derivate gains respectively. Note that when there is no leading vehicle, it will switch to unilateral car following mode:

$$a_n = k_d(s_{n-1} - s_0) + k_v(v_{n-1} - v_n) \quad (14)$$

where we want to control the relative space and speed between the current vehicle to its leader. s_0 is the desired space that can be set adaptively according to the car's speed, i.e., $s_0 = v_n T$ and T is the reaction time. This formula will be the same as shown in the Shladover car following model [24].

IV. METHOD

A. Bilateral Deep Reinforcement Learning for car following

In the car following scenario, if the lead vehicle speed oscillates, the oscillation can potentially magnify in the platoon of following vehicles leading to unstable and unsafe platoon behavior. Therefore, one of our four objectives is to make sure such oscillations are damped as soon as possible in the following platoon. We can define our problem following the bilateral control logic as suggested by [16]. According to [16], BCM chains (a chain of vehicles controlled by BCM) can make the perturbation from leading vehicles decay exponentially. Therefore, we augment our state space using bilateral sensing information which is described next.

B. State and Action Design

1) *State Space*: Based on [5], the RL-based car following model designs the state s_t as a 5-dimensional array: $(v_n(t), S_{n-1,n}(t), \Delta V_{n-1,n}(t), v_l, a_n(t-1))$ where $v_n(t)$ is the following vehicle speed at time step t , $S_{n-1,n}(t)$ is the clearance distance, $\Delta V_{n-1,n}(t)$ is the relative speed of vehicle $n-1$ with respect to vehicle n , v_l is the target speed on the current edge of the road, and $a_n(t-1)$ is the acceleration of the following vehicle n from last step. Unlike the CFM-based RL car-following model [5], we add two additional dimensions into our state space: clearance distance of the current vehicle n to its following vehicle $n+1$: $S_{n,n+1}(t)$; the relative speed of vehicle n with respect to vehicle $n+1$: $\Delta V_{n,n+1}(t)$. Therefore, our state space s_t is a 7-dimensional array:

$$s_t = (v_n(t), S_{n-1,n}(t), \Delta V_{n-1,n}(t), S_{n,n+1}(t), \Delta V_{n,n+1}(t), v_l, a_n(t-1)) \quad (15)$$

2) *Action Space*: Action space A is a continuous 1-dimensional space with range $(-3m/s^2, 3m/s^2)$, it represents the acceleration of the controlled RL vehicle.

C. Reward Function Design

We design the reward function based on safety, efficiency, and comfort. We evaluate the agents based on these three rewards as well as platoon stability.

1) *Safety* f_{safety} :We want to penalize vehicles with small TTC. At the same time, a vehicle with reasonable TTC should not be penalized. Thus, it is important to determine a threshold. According to [5], we use the following function as the safety component in the reward function:

$$f(ttc) = \begin{cases} \log\left(\frac{ttc}{4}\right) & 0 \leq ttc \leq 4 \\ 0 & \text{otherwise} \end{cases} \quad (16)$$

2) *Efficiency* (f_{eff}) :For the efficiency component, we use a log-normal distribution on time headway. Let $H \sim \text{Log-nmoral}(u, \sigma)$, then we have the following Probability density function (pdf) for H :

$$f(h) = \frac{1}{\sqrt{2\pi}h\sigma} \exp\left(-\frac{(\ln(h) - u)^2}{2\sigma^2}\right) \quad (17)$$

According to [5], based on the empirical data, we choose $u = 0.4226$, $\sigma = 0.4365$. As shown in [5], the maximum is located at some point around $h = 1.26$ with maximum value around 0.659. Although lower values of h can be tested, we use the same value as in [5] for fair comparison.

3) *Comfort* ($f_{comfort}$): Comfort component is based on jerk:

$$f(jerk) = -\frac{jerk^2}{3600} \quad (18)$$

We want the range of this reward component to be similar to others. In our simulation, the seconds per simulation step is 0.1s, thus the range of jerk is $(-60, 60)$. By dividing 3600, we can scale the range of $f(jerk)$ to $(-1, 0)$.

Therefore, our reward function is defined as the sum of these reward components which is used in CFM-based RL car-following model:

$$R_{CFM} = \omega_s * f_{safety} + \omega_e * f_{eff} + \omega_c * f_{comfort} \quad (19)$$

where $\omega_s, \omega_e, \omega_c$ are the weights for safety, efficiency, comfort functions. We set $\omega_s = \omega_e = \omega_c = 1$.

Following vehicle reward objective: Besides those three reward components in the front view car-following model, we would also add two additional back-view reward components:

- **Following Vehicle Safety** ($f_{safety-f}$) :Measure the safety of the following vehicle $n+1$ based on the TTC

of the current vehicle n and the following vehicle $n + 1$. The function is the same as the safety reward function (Equation 14) in the car-following model.

- **Following Vehicle Efficiency (f_{eff-f})** :Measure the efficiency of the following vehicle $n + 1$ based on the time headway of the following vehicle $n + 1$. The function is the same as the efficiency reward function (Equation15) in the car-following model.

Therefore, our reward function will be:

$$r = \omega_s * (f_{safety} + f_{safety-f}) + \omega_e * (f_{eff} + f_{eff-f}) + \omega_c * f_{comfort} \quad (20)$$

For a fair comparison, the weights are set as the same as in CFM model.

D. Learning Scheme

The learning agent interacts with the environment, which runs on the SUMO [20] simulator. We also use the FLOW [22] Python library to interact with the SUMO simulator.

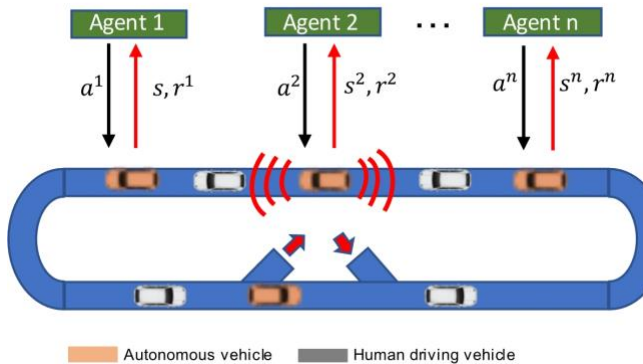


Figure 2. Distributed learning framework for bilateral reinforcement learning car following model. The road network is a single-lane closed-loop network with an entrance and exit ramp. During the training, the red vehicle will be driving on this closed-loop road. The gray vehicles will be generated by the simulator and flow into the network from the bottom-right ramp and leave the road by driving to the bottom-left ramp. The inflow rate of the human driving vehicle is 180 veh/h, and there are 5 autonomous vehicles in the network.

Training in a multi-agent scenario is challenging. Firstly, the state and action space will grow exponentially with the increase of autonomous vehicle agents by using a centralized training approach [22]. Secondly, we assume that there is no V2V or V2I communication so that each autonomous vehicle agent will only have a local observation.

We select the training network as the closed-loop network, which is shown in Figure 2. For the loop network, it's easy to add inflow and outflow, which is helpful for stabilizing the learning. Secondly, the agent can gather more experience in a loop network compared to an open road network.

One straightforward way is using a centralized multi-agent training framework, i.e., concatenating all the local observations together to put into the neural network (NN). However, the performance will decrease when the agent number increases.

Our decentralized multi-agent training framework is shown in Figure 2. There are n agents in the simulation scenario. Each agent is controlled in a distributed framework, i.e., each agent will only sense the leading and following vehicle, then get the corresponding observation s^i and the reward r^i . The policy is shared among all agents in the traffic network. The learned policy will generate the control action a^i for each agent.

V. EXPERIMENTS

A. Baseline selection

In the experiment, we consider the following baseline methods as shown in TABLE I. Firstly, we consider a single agent version of the BCM-RL method, named BCM-SARL in comparison with our method (BCM-MARL) to compare different learning frameworks. Secondly, we consider another car following RL baseline from[5]. Then we consider several non-learning car-following baselines which include BCM [16], Gipps [7], and IDM [23].

TABLE I.
Comparison of different baseline methods

methods	learning	safety	Efficiency	comfort	Stability
BCM-SARL	Single-agent	Yes	Yes	Yes	Yes
CFM-RL [5]	Single-agent	Yes	Yes	Yes	No
BCM [16]	No	No	No	No	Yes
Gipps [7]	No	No	Yes	No	No
IDM [8]	No	No	Yes	Yes	No
BCM-MARL	Multi-agent	Yes	Yes	Yes	Yes

B. Closed loop test experiment

Firstly, we test the trained agent in the same closed loop road network. In the training environment, there are five autonomous vehicle agents while we keep the same agent numbers in the testing scenario. These analyses are given below.

1) **Safety analysis:** Safety is an essential element for evaluating performance. Time to collision (TTC) is one surrogate indicator to represent safety. To compare the performance, we plot the TTC distribution for each method.

By comparing Figure 4. (a)-(c), we find that BCM's safety is better than the other two car-following baselines. BCM-SARL is slightly better than CFM-RL. Combined with a multi-agent training framework, the performance further improves.

2) **Efficiency analysis:** To compare the efficiency for different methods, we calculate the headway at each time step. At later time steps the vehicle platoon becomes more stable and headways become smaller.

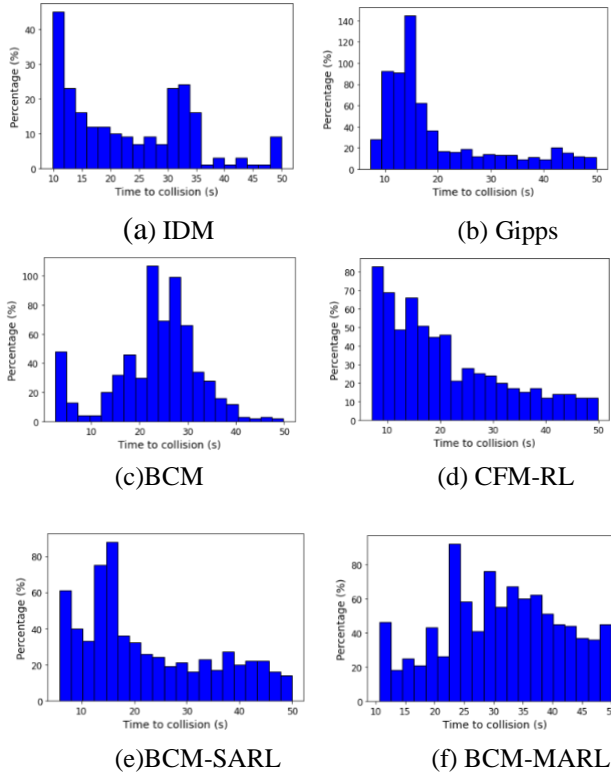


Figure 3. Distribution of TTC during closed loop car following. The target headway for each baseline is controlled as 1.26s. The more close to 0, the more unsafe.

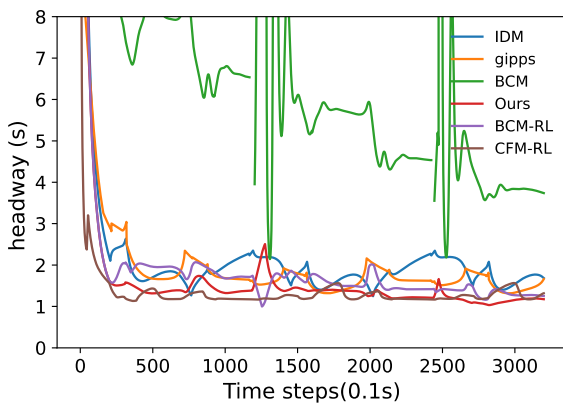


Figure 4. Headway comparison in closed loop car following scenario. The target headway is 1.26s.

From Figure 4. , we can find that BCM model tends to have unstable headway. Our method shows the lowest headways and hence most flow-efficient car following.

3) *Comfort analysis*: To visualize the jerk under a control policy, we plot the evolution of acceleration for each method given one episode.

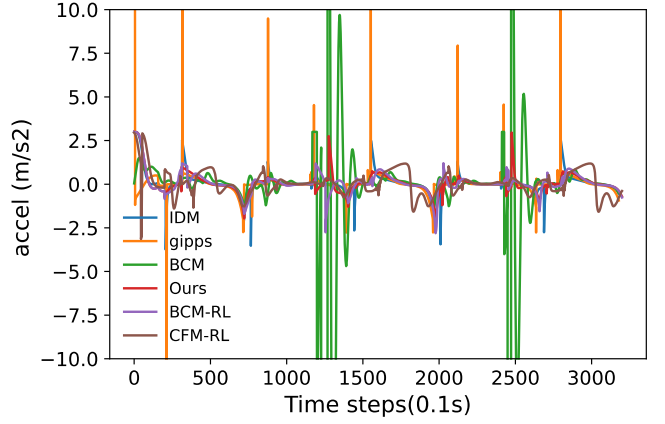


Figure 5. Acceleration comparison in closed loop car following scenario.

From Figure 5. , we can find that BCM and Gipps tend to have abrupt acceleration and hence higher jerk. We conjecture it's because these two models haven't considered bounds for action.

4) *Summary*: To make a comprehensive comparison, we select the average headway, jerk, TTC over one episode to measure the efficiency, comfort, and safety of each method.

TABLE II.
Comparison of different methods in closed loop test

Methods	Headway	Jerk	TTC
BCM-SARL	1.732	0.173	22.372
CFM-RL[5]	1.259	0.215	21.037
BCM [16]	2.175	0.341	28.970
Gipps [7]	1.755	1.400	19.714
IDM [8]	2.669	0.229	23.181
BCM-MARL	1.285	0.163	31.176

From TABLE II. , among the non-learning baselines we find that the Gipps model is more aggressive than IDM and BCM, as it has the smallest headway but the highest jerk. For learning-based models, comparing BCM-SARL and CFM-RL, we find that the BCM-SARL model sacrifices efficiency, i.e., uses higher headway, to achieve higher comfort and safety. As a result, they will have a smaller jerk and higher TTC. We also find our BCM-MARL method and CFM-RL are close to the target headway, i.e., 1.26 s, but the safety and comfort of our model are better than CFM-RL. In the next section we assess platoon stability across the models.

C. Perturbation test experiment

To complete the comparisons, we subject a platoon of vehicles on a straight road segment to traffic perturbation and visualize the platoon stability across all models. The focus of BCM, as a concept, is the suppression of the perturbation in the traffic. We visualize the behavior of the platoon using the space-time diagram shown in Figure 6. To create perturbations, we oscillate the speed of the leading vehicle as shown by the red profile. The follower vehicles are plotted in blue. We

compare the cases of the follower vehicles in the platoon being controlled by different car-following models as shown in Figures 7 a-f.

To make a comprehensive comparison, we also report the average headway, jerk, TTC over one episode to quantify the efficiency, comfort, and safety for each method. Note that because TTC values are very large due to the minor speed variations in this experiment, we compare safety using the log of TTC as in Equation 15.

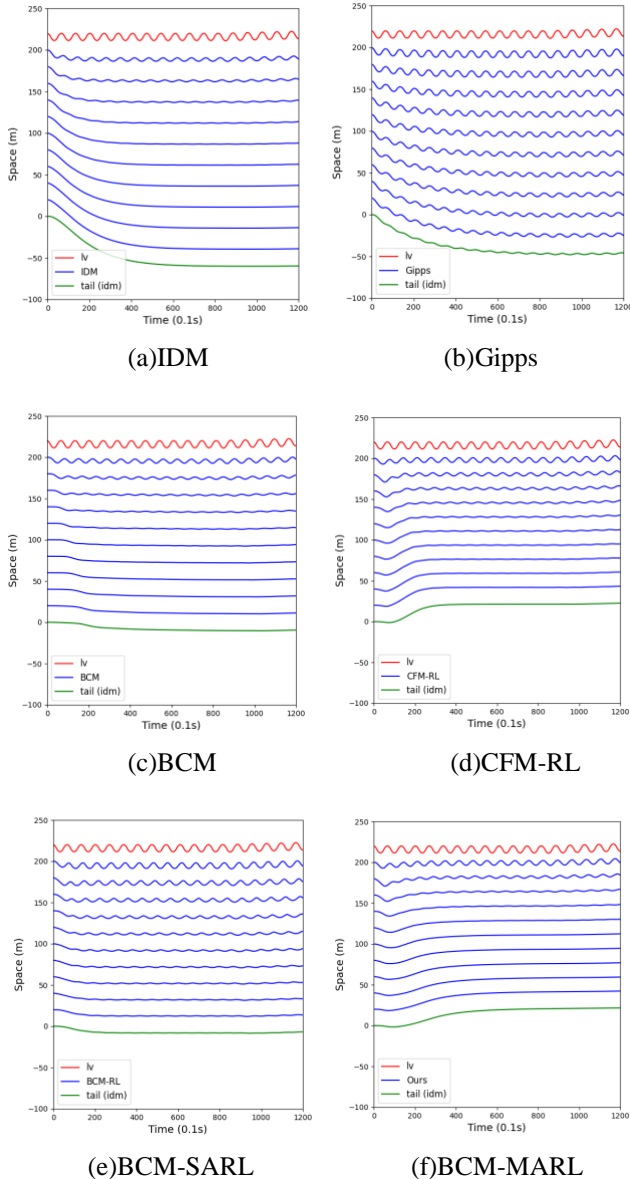


Figure 6. Perturbation of different controllers, larger oscillation means larger perturbation. The following vehicles move at speed of 20m/s, the number of BCM vehicle is 10. The y axis is the space which represent the relative position corresponding to given time steps. The tail vehicle is controlled by IDM because there is no vehicle behind to use BCM. For a fair comparison, we select IDM as the tail vehicle for all methods.

Methods	Headway	Jerk	Safety
BCM-SARL	1.368	0.650	0.668
CFM-RL [5]	1.340	0.352	0.586
BCM [16]	1.361	0.300	0.422
Shladover [24]	0.994	0.289	0.579
Gipps [7]	1.587	1.610	0.560
IDM [8]	1.675	0.236	0.491
BCM-MARL	1.180	0.057	0.827

TABLE IV.
Comparison of different methods in perturbation test (target headway=0.8s)

Methods	Headway	Jerk	Safety
BCM-SARL	1.012	0.392	0.491
CFM-RL [5]	0.992	0.278	-1.661
BCM [16]	1.361	0.300	0.422
Shladover[24]	0.994	0.289	0.579
Gipps [7]	1.587	1.610	0.560
IDM [8]	1.158	0.368	-1.301
BCM-MARL	0.830	0.345	0.581

Based on TABLE III. and Figure 7, we observe two effects: how quickly the oscillations dampen and what is the resulting performance in terms headway (is the platoon compact or spaced up), as well as jerk and TTC. Ideally, a better model would yield faster dampening of oscillations and tighter platoons with shorter headways. Further, lower jerk and higher log TTC are better. Visually from Figure 7 and numerically from Table III, we find that BCM models in general naturally dampen perturbations better. RL models in general achieve more compact platoons and shorter headways than non-learning methods. BCM MARL outperform CFM-RL because CFM-RL does not account for the effect of the follower vehicle, and hence exhibit less chain stability, which also reduces efficiency as well. BCM MARL further enhances chain stability over BCM SARL indicating better learning potential. We can find that our multi-agent BCM-MARL model is better than single-agent BCM-RL in terms of headway, jerk, and safety.

Secondly, in TABLE IV. we decrease the target headway to 0.8, which is below the mode headway of human driving [5]. Firstly, the Shladover, Gipps, BCM models' formulas are independent on target headway so that they keep the same results. We observe CFM-RL[5] can achieve smaller headway than humans, but at the expense of lower safety. On the other hand, BCM-MARL can achieve smaller headway than human driving while achieving better safety and comfort, demonstrating that it outperforms human driving performance.

Overall, our model outperforms all the other baselines in the perturbation test. While Shladover achieves shortest headways, it does so at the expense of higher jerk and lower safety compared to BCM-MARL.

TABLE III.

Comparison of different methods in perturbation test (target headway=1.26s)

VI. CONCLUSIONS AND DISCUSSION

In this paper, we designed the bilateral deep reinforcement learning framework for car following control. We find that our framework has better performance than human driving models. It is the most effective perturbation damper among these models. Also, it is in the top place in other metrics, i.e., safety, efficiency, comfort.

Notice that we also compare our decentralized multi-agent training framework with single-agent training of both CFM and BCM DDPG. We can also find that multiagent learning setting can further boost the performance.

In the future, we will add following target speed into the objective function. However, there would be challenges because more complicated objectives will create local optimal issue in the learning phase. Also, we will investigate how to make our autonomous vehicle agent becomes more adaptable, i.e., if the leading vehicle violates the speed limit, the follower vehicle will follow the speed limit rather than the leader. It is also worth mentioning that for bilateral deep RL models, their average headway to the front vehicles is slightly worse than CFM whose average headway stays exactly at the optimal value. We suspect this is a trade off since the bilateral RL models also need to maintain a good headway of its following vehicle.

REFERENCES

- [1] M. Treiber and A. Kesting, "Traffic flow dynamics," *Traffic Flow Dynamics: Data, Models and Simulation*, Springer-Verlag Berlin Heidelberg, 2013.
- [2] A. R. Kreidieh, C. Wu, and A. M. Bayen, "Dissipating stop-and-go waves in closed and open networks via deep reinforcement learning," in *2018 21st International Conference on Intelligent Transportation Systems (ITSC)*. IEEE, 2018, pp. 1475–1480.
- [3] T. Shi, P. Wang, X. Cheng, C.-Y. Chan, and D. Huang, "Driving decision and control for autonomous lane change based on deep reinforcement learning," *arXiv preprint arXiv:1904.10171*, 2019.
- [4] P. Wang, C.-Y. Chan, and A. de La Fortelle, "A reinforcement learning based approach for automated lane change maneuvers," in *2018 IEEE Intelligent Vehicles Symposium (IV)*. IEEE, 2018, pp. 1379–1384.
- [5] M. Zhu, Y. Wang, Z. Pu, J. Hu, X. Wang, and R. Ke, "Safe, efficient, and comfortable velocity control based on reinforcement learning for autonomous driving," *Transportation Research Part C: Emerging Technologies*, vol. 117, p. 102662, 8 2020. [Online]. Available: <http://dx.doi.org/10.1016/j.trc.2020.102662>
- [6] D. C. Gazis, R. Herman, and R. W. Rothery, "Nonlinear follow-the-leader models of traffic flow," *Operations research*, vol. 9, no. 4, pp. 545–567, 1961.
- [7] P. G. Gipps, "A behavioural car-following model for computer simulation," *Transportation Research Part B: Methodological*, vol. 15, no. 2, pp. 105–111, 1981.
- [8] M. Treiber, A. Hennecke, and D. Helbing, "Congested traffic states in empirical observations and microscopic simulations," *Physical review E*, vol. 62, no. 2, p. 1805, 2000.
- [9] Z. He, L. Zheng, and W. Guan, "A simple nonparametric car-following model driven by field data," *Transportation Research Part B: Methodological*, vol. 80, pp. 185–201, 2015.
- [10] L. Chong, M. M. Abbas, A. Medina Flintsch, and B. Higgs, "A rule-based neural network approach to model driver naturalistic behavior in traffic," *Transportation Research Part C: Emerging Technologies*, vol. 32, pp. 207–223, 2013. [Online]. Available: <https://www.sciencedirect.com/science/article/pii/S0968090X12001210>
- [11] M. Zhou, X. Qu, and X. Li, "A recurrent neural network based microscopic car following model to predict traffic oscillation," *Transportation research part C: emerging technologies*, vol. 84, pp. 245–264, 2017.
- [12] T. Mikolov, M. Karafiat, L. Burget, J. Černocký, and S. Khudanpur, "Recurrent neural network based language model," in *Eleventh annual conference of the international speech communication association*, 2010.
- [13] D. Silver, A. Huang, C. J. Maddison, A. Guez, L. Sifre, G. Van Den Driessche, J. Schrittwieser, I. Antonoglou, V. Panneershelvam, M. Lanctot et al., "Mastering the game of go with deep neural networks and tree search," *nature*, vol. 529, no. 7587, pp. 484–489, 2016.
- [14] V. Mnih, K. Kavukcuoglu, D. Silver, A. Graves, I. Antonoglou, D. Wierstra, and M. Riedmiller, "Playing atari with deep reinforcement learning," *arXiv preprint arXiv:1312.5602*, 2013.
- [15] M. Zhu, X. Wang, and Y. Wang, "Human-like autonomous car-following model with deep reinforcement learning," *Transportation research part C: emerging technologies*, vol. 97, pp. 348–368, 2018.
- [16] L. Wang and B. K. P. Horn, "On the chain stability of bilateral control model," *IEEE Transactions on Automatic Control*, vol. 65, no. 8, pp. 3397–3408, 8 2020.
- [17] R. S. Sutton, A. G. Barto et al., *Introduction to reinforcement learning*. MIT press Cambridge, 1998, vol. 135.
- [18] T. P. Lillicrap, J. J. Hunt, A. Pritzel, N. Heess, T. Erez, Y. Tassa, D. Silver, and D. Wierstra, "Continuous control with deep reinforcement learning," 2019.
- [19] K. Vogel, "A comparison of headway and time to collision as safety indicators," *Accident Analysis & Prevention*, vol. 35, no. 3, pp. 427–433, 2003. [Online]. Available: <https://www.sciencedirect.com/science/article/pii/S0001457502000222>
- [20] P. A. Lopez, M. Behrisch, L. Bicker-Walz, J. Erdmann, Y.-P. Flötteröd, R. Hilbrich, L. Lücken, J. Rummel, P. Wagner, and E. Wießner, "Microscopic traffic simulation using sumo," in *The 21st IEEE International Conference on Intelligent Transportation Systems*. IEEE, 2018. [Online]. Available: <https://elib.dlr.de/124092/>
- [21] C. Wu, A. Kreidieh, K. Parvate, E. Vinitsky, and A. M. Bayen, "Flow: A modular learning framework for autonomy in traffic," 2020..
- [22] R. Lowe, Y. I. Wu, A. Tamar, J. Harb, O. P. Abbeel, and I. Mordatch, "Multi-agent actor-critic for mixed cooperative-competitive environments," in *Advances in neural information processing systems*, 2017, pp. 6379–6390.
- [23] M. Treiber, A. Hennecke, and D. Helbing, "Congested traffic states in empirical observations and microscopic simulations," *Physical Review E*, vol. 62, no. 2, p. 1805–1824, 8 2000. [Online]. Available: <http://dx.doi.org/10.1103/PhysRevE.62.1805>
- [24] Milanés, V., & Shladover, S. E. (2014). Modeling cooperative and autonomous adaptive cruise control dynamic responses using experimental data. *Transportation Research Part C: Emerging Technologies*, 48, 285-300